Pergamon

Atmospheric Environment Vol. 29, No. 3, pp. 449–453, 1995

1352–2310/95 $9.50 + 0.00

1352–2310(94)00258-4

TECHNICAL NOTE

CORRECTIONS FOR PARTICLE LOSSES AND SIZING ERRORS DURING AIRCRAFT AEROSOL SAMPLING USING A ROSEMOUNT INLET AND THE PMS LAS-X

V. L. FOLTESCU and E. SELIN

Department of Physics, University of Göteborg and Chalmers University of Technology, S-412 96 Göteborg, Sweden

and

M. BELOW

Centre of Radiation Protection and Radio Ecology, University of Hannover, Herrenhäuser Str. 2, D-30419, Germany

(*First received* 14 *March* 1994 *and in final form* 18 *August* 1994)

Abstract—*In situ* flight measurements of accumulation mode aerosol particles were performed in the upper troposphere during the 1991/1992 EASOE (European Arctic Stratospheric Ozone Experiment). On-line number size distributions were obtained by using an optical particle counter, the PMS LAS-X. Support data, like ozone mixing ratios, and meteorological as well as flight parameters were collected simultaneously. The present study analyses the particle sampling system used aboard the Transall aircraft. A correction algorithm for particle losses and sizing errors is developed based on calculations. A corrected number size distribution is compared with measurements reported in the literature.

Key word index: *In situ* aircraft measurement, stratospheric aerosol, tropopause folding, accumulation mode particles, aircraft sampling, particle losses, sizing errors.

INTRODUCTION

Extensive flight measurements of accumulation mode aerosol particles in the upper troposphere were performed during the 1991/1992 EASOE (European Arctic Stratospheric Ozone Experiment) from a large aircraft platform, Transall C-160. The size segregated number concentrations of particles between 0.10 and 0.91 μm were measured on-line, with a time resolution of 30 s, by operating an optical particle counter from the Particle Measuring Systems Inc. (PMS), type LAS-X. Flight and meteorological parameters and ozone mixing ratios were measured simultaneously, with the same time resolution.

Accumulation mode particles are known to influence the radiative transfer in the atmosphere and the acidic wet deposition. They are also known to play an important role in cloud formation and, if they are located in the stratosphere, they may be involved in heterogeneous chemistry leading to ozone depletion. Therefore, measurements of the accumulation mode particles in both troposphere and stratosphere are of great importance.

A great deal of scientific effort in aerosol science concerns determination of particle losses during sampling from aircraft. The losses are size-dependent and very difficult to assess. The present paper proposes to examine the performances of the particle sampling system and the sizing instrument used aboard the Transall aircraft. It attempts to assess the size-dependent losses of the particles in the aspirated system. Corrections for these sampling artefacts are to be taken into account in the future data analysis.

DESCRIPTION OF THE ROSEMOUNT INLET AND SAMPLING SYSTEM

The aerosol was drawn inside the aircraft through a Rosemount inlet, an inlet which is normally used for temperature and humidity measurements outside aircraft. The Rosemount inlet had the official installation certificate according to the requirements of the air traffic regulations and was approved also for aerosol measurements. It can be seen from Fig. 1 that the inlet is essentially a T-piece, that implies 90° aspiration from the airstream in order to bring the sampling volume inside the aircraft. The sampling line, consisting of various tubes, is divided into three sections. The first section is prior to the 90° aspiration. This section is in reality rectangular but approximated with a cylindrical tube for the convenience of efficiency calculations. The second section leads the aerosol inside the aircraft and then through a 90° bend to the vicinity of the instrumental rack. The third section consists of a tube that is placed isoaxially inside the second tube and leads the aerosol through a 90° bend to the OPC. All the sampling lines are lying at approximately the same horizontal level with respect to the Earth. The inlet parameters are given in Table 1, where L_i = length of inlet and/or tubing and D_i = diameter of inlet or tube. The Rosemount inlet is 11 cm far away from the aircraft skin and is placed on the lower front part of the fuselage, on one side. This is in accordance with the recommendations of King (1984) in order to perform representative sampling. Minimum air flow distortion and vortices are expected at this location of the probe.

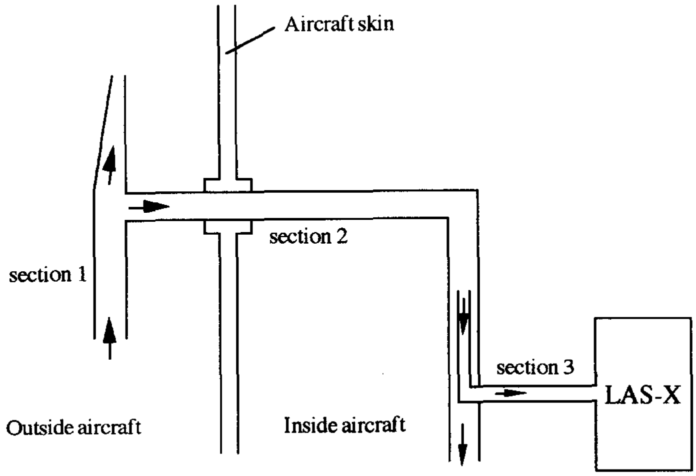

Fig. 1. Schematic picture of the aerosol sampling system.

Table 1. Inlet and particle parameters used to calculate the overall sampling efficiency

Parameter	Section one	Section two	Section three
L_i (cm)	5.0	200.0	25.0
D_i (cm)	1.0	1.0	0.05
U_w (m s^{-1})	120.0	120.0	2.4
U_i (m s^{-1})	120.0	2.4	15.0
R	1.0	50.0	0.16
Stk (d_p=0.1 μm)	0.0035	0.0035	0.0015
Stk (d_p=1.0 μm)	0.0902	0.0902	0.0401
Re	41,770	835.0	227.0

CALCULATION OF PARTICLE LOSSES

Particle losses in the sampling system are always of outmost concern when performing aircraft measurements. Wind tunnel measurements at the simulated flight conditions would be decisive in establishing the true effectivity of the sampling system. When access to such special facilities is not possible, estimations about the sampling efficiency rest on theoretical and semiempirical relations found in the literature and on comparisons with other measurements. This is also the case for the present study.

The overall particle sampling efficiency, E_s, of an inlet is often given as a product of three different efficiencies (Hangal and Willeke, 1990):

$$E_s = E_a E_r E_t$$

where E_a is the aspiration efficiency, E_r is the entry efficiency, and E_t is the transmission efficiency. Equations for calculating the different efficiencies have been determined from experimental data at various conditions. Such experiments have been performed in wind tunnels, at moderate wind speeds and standard atmospheric pressure and temperature. Eventually, theories have been put forward to explain the experimental findings. In this way, semi-empirical unified models have been created, see for example Vincent (1989). When equations reported in the literature are to be applied to aircraft sampling one is confronted with a dilemma: may or may not the equations be applicable to evaluate the losses at the high velocities, low pressures and low temperatures encountered during flights. There is an extreme lack of measurements to verify if the equations that govern particle losses work at flight conditions. This has also been pointed out at the Airborne Aerosol Inlet Workshop in 1991 (Baumgardner and Huebert, 1993). The present paper is an attempt to validate some of the efficiency equations, at least for the special conditions in the present experiment. Efficiency calculations are made separately for each section and an overall sampling efficiency is obtained as

$$E_s = E_{s1} E_{s2} E_{s3}.$$

Owing to the fact that stratospheric aerosol was repeatedly encountered at the cruising altitude, the calculations are made for supercooled stratospheric particles, assumed to be made of 70% H_2SO_4 and 30% H_2O, thus having a particle density, $\rho_p = 1.59$ g cm^{-3}. The temperature used is 223 K and the pressure 370 mb at the cruising altitude. Particle parameters, such as particle relaxation time, τ, and Stokes number, Stk, are highly influenced by the extreme temperature and pressure conditions, compared to the more agreeable ground conditions. Some of the parameters used in the efficiency computations are shown in Table 1, in which U_w is wind (air stream) velocity, U_i is inlet air velocity, R is the ratio between wind velocity and inlet air velocity, Stk is the dimensionless Stokes number for curvilinear particle motion and Re is the dimensionless flow Reynolds number that characterises the type of flow: turbulent flow for $Re > 4000$ and laminar flow for $Re < 2000$. The formulae used for efficiency calculations are summarised in Table 2.

Section one

The aspiration and entry efficiencies, E_a and E_r of section one are set to 1, as the first approximation. It is assumed that the particle concentration incident to the inlet face, and the

Table 2. Equations used for sampling efficiency calculations

Equation		Reference
(1)	$E_{ts} = \exp(-4.7\,K^{0.75})$	Okazaki and Willeke (1987)
(2)	$E_{td} = \exp[-(4\,L_i D)/(D_i U_i \delta)]$	Hinds (1982)
(3)	$E_a = 1 + (R\cos\theta - 1)\left[1 - \dfrac{1}{1 + 2.1\,Stk(\cos\theta + 4\,R^{1/2}\sin^{1/2}\theta)}\right]$	Vincent *et al.* (1986)
(4)	$E_{ti} = 1 - \dfrac{0.5\pi S\sqrt{2D_i S - S^2}}{\pi\left(\dfrac{D_i}{2}\right)^2}$	—
(5)	$E_{td} = 1 - 5.50\,\mu^{2/3} + 3.77\,\mu$, for $\mu < 0.007$	
(6)	$E_{td} = 0.819\exp(-11.5\,\mu) + 0.0975\exp(-70.1\,\mu) + 0.0325\exp(-179\,\mu)$, for $\mu > 0.007$	Hinds (1982)
(7)	$E_{tb} = \exp(-2.823\,Stk\,\phi)$	Pui *et al.* (1987)
(8)	$E_a = 1 + (R-1)\,[1 + 0.506\,R^{1/2}Stk^{-1}]^{-1}$	Zhang and Liu (1989)

Note: Parameters not defined in the text.
K = inlet deposition parameter; δ = thickness of diffusion boundary layer, originally introduced by Fuchs; μ = dimensionless deposition parameter; θ = angle of sampling; ϕ = angle of the bend in radians; S = stopping distance; D = diffusion coefficient.

ambient particle concentration are equal, meaning that the ratio of the two concentrations, by definition equal to E_a, is 1. $E_r = 1$ means that the inlet is approximated with a perfectly sharp-edged inlet, i.e. having no particle bounce from the tip of the inlet. In reality the inlet is more blunt than sharp. The transmission efficiency is usually divided into three components. One is due to losses by gravitational settling in the boundary layer of the inlet, E_{ts}; the second is due to impaction losses, E_{ti}; and the third is due to deposition on walls by diffusion, E_{td}. E_{ts} and E_{td} for section one are calculated from relations found in the literature [see Table 2, equations (1) and (2)]. E_{ti} is approximated with 1, assuming that impaction in section one is insignificant. The overall sampling efficiency of section one is displayed as a dotted curve in Fig. 2.

Section two

The aspiration efficiency for section two was difficult to assess. Several approaches have been tried. The equation of Durham and Lundgren (1980) for sampling from 0 to 90° was restricted. It could not be applied for 90° sampling together with $R \neq 1$. The equation of Laktionov (1973) for 90° sampling, valid for at least $1.25 \leqslant R \leqslant 6.25$ and $0.003 \leqslant Stk \leqslant 0.2$ yielded unphysical negative values. The equation of Vincent *et al.* (1986), see equation (3) in Table 2, experimentally tested for $0.67 \leqslant R \leqslant 2$ and $0.1 \leqslant Stk \leqslant 14.5$, was finally applied for an angle $\theta = 90°$. The aspiration efficiency was calculated to 83% for $d_p = 0.1\ \mu$m and 16% for $d_p = 1\ \mu$m. E_{ts} is calculated for section two by use of equation (1) in Table 2. E_r is set to 1. The approach to estimate the impaction losses, and thus E_{ti} for the 90° sampling into section two is to define a critical trajectory for the particles and say that all particles will impact if their trajectories are passing through an impaction region which is within one stopping distance from the wall opposite to their incoming direction. The fraction of particles that impact on the wall is then given by the ratio between the cross-sectional area of the impaction region and the cross-sectional area of the tube. The area of impaction may be approximated with that of one half ellipse. The relation used to estimate E_{ti} is given in Table 2, equation (4). E_{td} for section two is given by equations (5) and (6). An additional efficiency must be calculated for section two, owing to the 90° bend which is subject to impaction losses. The transmission efficiency, of the bend E_{tb}, is calculated by use of the simple relation, equation (7), in Table 2.

The efficiency curve for sections 1 and 2 together is seen as the dashed curve in Fig. 2.

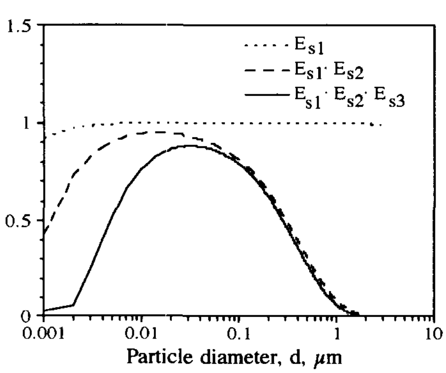

Fig. 2. Curves for particle penetration through the three sections of the sampling system. The continuous line represents the overall sampling efficiency: 1 corresponds to 100% penetration efficiency.

Section three

The aspiration efficiency, E_a, for the isoaxial sampling in section three is calculated by use of equation (8) in Table 2. The entry efficiency, E_r is set to 1. E_{ts} and E_{td}, are estimated by using equations (1), (5) and (6) in Table 2. The 90° bend of the tube in section three is subject to impaction losses. These losses are accounted for by using equation (7).

The calculated overall efficiency of the entire sampling system is drawn with a continuous line in Fig. 2.

CORRECTIONS FOR SIZING ERRORS

Shrinkage of particles

Concomitantly with the particle losses in the sampling system, the particles that pass through the sampling lines undergo physical changes. The aerosol is subjected to changing conditions of temperature and pressure. The aerosol sample is heated by the heat transfer from the significant temperature difference between the inside and outside of the aircraft. The temperature and pressure of the aerosol are also expected to increase due to compressive heating (Porter *et al.*, 1992). Changing the temperature and pressure of the aerosol sample causes a reduction of relative humidity in the sampling line compared to the ambient values, and the particles evaporate to some smaller sizes. In the present study, the shrinkage is estimated to 10%. This corresponds to the reduction of particle diameters when particles (consisting of sulphuric acid and water) readjust from equilibrium sizes at 225 K outside the aircraft to new equilibrium sizes at 273 K at the instrument. The shrinkage was calculated using the tabulated values of Steele and Hamill (1981). An extrapolation was required to obtain the value for 273 K, since the changes in particle sizes were tabulated for the range 190–260 K.

Sizing errors with the LAS-X

The physical principle employed by the PMS LAS-X is light scattering by individual aerosol particles. The optical particle diameter is determined from the amount of light scattered into a photo detector, as the particle passes through a laser beam. The scattered light intensity depends not only on particle size, but also on shape and on particle refractive index, *m*, which is connected to the chemical composition of the particles. Provided that the measured particles are spherical and have the same refractive index as the particles used for calibration, the optical diameter indicated by the instrument equals the geometric particle diameter. If the measured particles have lower refractive indexes, they scatter less light and the instrument will probably undersize them. Accurate measurement of the number concentration with an optical particle counter requires knowledge of *m*. For example, if particles are made of sulphuric acid in aqueous solution, $m = 1.44 - 0.0i$ (Steele and Hamill, 1981). For the present study the LAS-X had been calibrated with polystyrene latex particles (PSL), having $m = 1.59 - 0.0i$. During the flight missions we encountered repeatedly stratospheric sulphuric acid particles by flying into tropopause fold regions. This was established by the chemical analysis of the particles. Sulphate was the major chemical component in the particles collected by low pressure impactors. The impactors were operated simultaneously with the LAS-X, however, using a separate sampling line. A sizing error is expected at the LAS-X while sampling stratospheric sulphuric acid particles. This is due to the difference in refractive index named earlier.

In order to correct for the sizing error we used the nonlinear relation found by Hering and McMurry (1991) between the indicated and the actual geometric particle diameter. Hering and McMurry have described the response of the PSL-calibrated LAS-X to monodisperse oleic acid particles, with $m = 1.46 - 0.0i$, thus very close to the refractive index of sulphuric acid. For the correction purpose, the experimental data obtained by Hering and McMurry have been fitted by a polynomial function. This function is used in the present study to correct for the error of indicated particle diameters in the range 0.25–0.65 μm. No correction is applied for the size ranges below 0.25 μm, because no experimental data points exist for that range in the study of Hering and McMurry. In that case, the undersizing error that might be the result has been evaluated as 9% at most. This must be kept in mind when studying the reconstructed ambient size distributions.

RESULTS AND CONCLUSION

Table 3 lists the corrected size ranges and the calculated sampling efficiencies. In the second column are shown the LAS-X measured (indicated) size ranges. In the third column appear the corrected, ambient particle diameters. The overall sampling efficiency decreases drastically with increasing particle size. Less than 10% of the micron and supermicron particles are able to reach the instrument. The supermicron particles are also affected by poor sampling statistics which limits the size range of the investigated aerosol. Consequently, the upper end of the reconstructed size distribution is taken below 1 μm.

The efficiency corrections from Table 3 have been applied to reconstruct the size distribution of the stratospheric aerosol (in the accumulation size range) measured within a tropopause fold region in 17 February 1992 around 49°N, 10°E (see Fig. 3). For comparison reasons this distribution is displayed together with the levels of one distribution obtained by Wilson *et al.* (1993) for the 13 km aerosol along the 45° northern latitude, from 13 February 1992. Aerosol measurements in the remote atmosphere are extremely sparse and comparisons are difficult to make. It is not straightforward to assume an evenly distributed stratospheric aerosol (e.g. between 45°N and 49°N) and steadiness of the number concentration and size distribution in time (e.g. between 13 February 1992 and 17 February 1992). Despite the difficulties in comparing, we observe a general agreement between the two measurements. The mixing ratios of the first, fourth and eighth size ranges agree quantitatively well (within 10%). The magnitude of the accumulation mode aerosol is rather similar as well. The least agreement is for particles of about 0.5 μm diameter. A predominant mode, centered at around 0.5 μm is seen in the reconstructed size distribution of the present study. However, this is not very peculiar. Other investigators have predicted (Friend, 1966) or found (e.g. Hofmann *et al.*, 1983) a mode below 1 μm. This is regarded as typical for stratospheric aerosol after major volcanic eruptions. Our measurements were performed seven months after the eruptions of Mount Pinatubo on the Philippines. Wilson *et al.* (1993) have also reported a size distribution with a significant mode at around 0.5 μm, however, at a higher altitude, 18 km.

Table 3. Uncorrected/corrected size intervals and corresponding efficiency corrections for particles aspirated inside the aircraft and measured by the LAS-X

Size range (Channel)	Indicated d_p	Ambient d_p	Mean d_p	Efficiency
1	0.09–0.11	0.10–0.12	0.11	0.77
2	0.11–0.15	0.12–0.17	0.14	0.71
3	0.15–0.20	0.17–0.22	0.19	0.63
4	0.20–0.25	0.22–0.28	0.26	0.54
5	0.25–0.30	0.31–0.40	0.35	0.41
6	0.30–0.40	0.40–0.62	0.51	0.27
7	0.40–0.50	0.62–0.79	0.70	0.15
8	0.50–0.65	0.79–0.91	0.85	0.10

Note: Particle diameters, d_p, are given in μm.

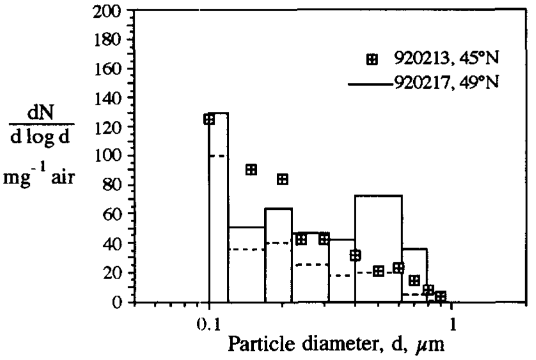

Fig. 3. Stratospheric particle number distribution: efficiency corrected (—), and uncorrected (- - -). The squares represent levels on one distribution reported by Wilson *et al.* (1993).

It is not conceivable that a too steep efficiency curve for the sizes representing the mode would be responsible for the appearance (the 0.5 μm-mode) of the reconstructed size distribution. If the same efficiency and size corrections, discussed earlier in the text, are applied to the measured size distributions of typical free tropospheric aerosols (apart from possible different input parameters, such as refractive index, particle density and relative humidity), one cannot identify any tendency of increasing modes at 0.5 μm. Instead, the number distributions follow roughly an inverse power law distribution, as expected by Hinds (1982). Thus, it is most likely that the mode identified in the number distribution of the stratospheric aerosol is real and is not a computational artefact.

Considering the consistency of the results and the general agreement with other measurements we are inclined to think that the equations used in the present study have been sufficient to describe, at least to a first approximation, the complex changes that the aerosol experienced during sampling. In conclusion, the efficiency calculations, which were based on equations given in the literature, are considered reliable, at least for the special conditions in the present experiment.

Acknowledgements—The Swedish participation was made possible by means of two grants from Adlerbertska Research Fund and Knut & Alice Wallenberg's Foundation, which are greatly acknowledged. The University of Hannover was funded by the German Ministry of Science and Technology, grant 01 V0Z 29A-8, while the aircraft operation costs were supported by the EC.

REFERENCES

Baumgardner D. and Huebert B. (1993) The airborne aerosol inlet workshop: meeting report. *J. Aerosol Sci.* **24**, 835–846.

Durham M. D. and Lundgren D. A. (1980) Evaluation of aerosol aspiration efficiency as a function of Stokes number, velocity ratio and nozzle angle. *J. Aerosol Sci.* **11**, 179–188.

Friend J. P. (1966) Properties of the stratospheric aerosol. *Tellus* **18**, 465–473.

Hangal S. and Willeke K. (1990) Overall efficiency of tubular inlets sampling at 0–90 degrees from horizontal aerosol flows. *Atmospheric Environment* **24A**, 2379–2386.

Hering S. V. and McMurry P. H. (1991) Optical Counter Response to Monodisperse Atmospheric Aerosols. *Atmospheric Environment* **25A**, 463–468.

Hinds W. C. (1982) *Aerosol Technology. Properties, Behaviour, and Measurement of Airborne Particles*, Chapters 7.4 and 14. Wiley, New York.

Hofmann D. J., Rosen J. M., Reiter R. and Jäger H. (1983) Lidar- and balloon-borne particle counter comparisons following recent volcanic eruptions. *J. geophys. Res.* **88**(C6), 3777–3782.

King W. D. (1984) Airflow and particle trajectories around aircraft fuselages. *J. atmos. ocean. Technol.* **1**, 5–13.

Laktionov A. B. (1973) Aspiration of an aerosol into a vertical tube from a flow transverse to it. *Fizika Aerozoley* **7**, 83–87 (Translation from Russian: AD-760 947, Foreign Technology Division, Wright-Patterson Air Force Base, Dayton, OH, U.S.A.)

Okazaki K. and Willeke K. (1987) Transmission and deposition behaviour of aerosols in sampling inlets. *Aerosol Sci. Technol.* **7**, 275–283.

Porter J. N., Clarke A. D., Ferry G. and Pueschel R. F. (1992) Aircraft studies of size-dependent aerosol sampling through inlets. *J. geophys. Res.* **97**(D4), 3815–3824.

Pui D. Y. H., Romay-Novas F. and Liu B. Y. H. (1987) Experimental study of particle deposition in bends of circular cross section. *Aerosol Sci. Technol.* **7**, 301–315.

Steele H. M. and Hamill P. (1981) Effects of temperature and humidity on the growth and optical properties of sulphuric acid–water droplets in the stratosphere. *J. Aerosol Sci.* **12**, 517.

Vincent J. H. (1989) *Aerosol Sampling Science and Practice*, Chapter 6.6. Wiley, New York.

Vincent J. H., Stevens D. C., Mark D., Marshall M. and Smith T. A. (1986) On the aspiration characteristics of large-diameter, thin-walled aerosol sampling probes at yaw orientations with respect to the wind. *J. Aerosol Sci.* **17**, 211–224.

Wilson J. C., Jonsson H. H., Brock C. A., Toohey D. W., Avallone L. M., Baumgardner D., Dye J. E., Poole L. R., Woods D. C., DeCoursey R. J., Osborn M., Pitts M. C., Kelly K. K., Chan K. R., Ferry G. V., Loewenstein M., Podolske J. R. and Weaver A. (1993) *In situ* observations of aerosol and chlorine monoxide after the 1991 eruption of Mount Pinatubo: effect of reactions on sulfate aerosol. *Science* **261**, 1140–1143.

Zhang Z. Q. and Liu B. Y. H. (1989) On the empirical fitting equations for aspiration coefficients for thin walled sampling probes. *J. Aerosol Sci.* **20**, 713–720.